

Topic number: 10.

## CHARACTERIZATION OF A HIGH PRESSURE CYLINDRICAL CATHODE/MOVEABLE ANODE SOURCE

Greenan J<sup>1\*</sup>, Mahony CMO<sup>1</sup>, Maguire PD<sup>1</sup>, Mariotti D<sup>1</sup>, Marić D<sup>2</sup>, Petrović Z.Lj<sup>2</sup>

<sup>1</sup> Nanotechnology & Integrated Bio-Engineering Centre (NIBEC), University of Ulster, Northern Ireland

<sup>2</sup> Gaseous Electronics Laboratory, Institute of Physics, Belgrade, Serbia

\* [Greenan-j@email.ulster.ac.uk](mailto:Greenan-j@email.ulster.ac.uk)

Cylindrical tube discharges are used in a wide variety of applications in plasma processing and show a promising approach to technology advancements in biomedical applications [1]. High pressure tubular cathode plasmas with molecular (e.g. C<sub>2</sub>H<sub>2</sub>, CH<sub>4</sub>) or atmospheric gases have potential applications in 3D thin film coatings [2], plasma gas sensors [3] and nanoparticle generation. Determining the optimal design for reliable operation, ignition and control requires considerable development for each application. Here we present aspects of electrical and optical characterisation of a plasma device with potential in all three applications areas.

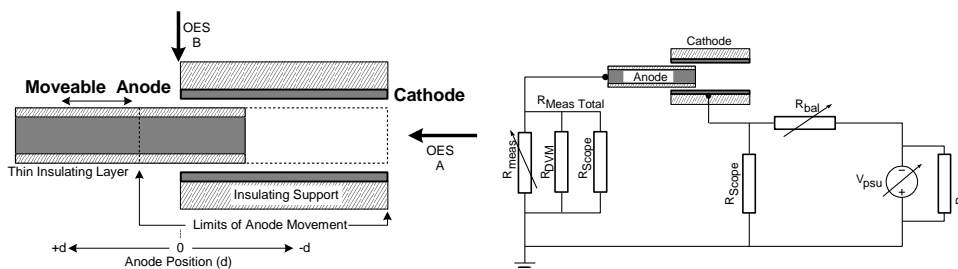


**Figure 1: Source schematic and electrical circuit**

The plasma source Fig (1) was DC driven and operated at static argon pressures >100mTorr. It consists of a 10mm long stainless steel cylindrical tube cathode of 2.6mm OD & 1.8mm ID, housed in an insulating support. The anode is a 1mm OD stainless steel rod with a thin insulating layer on the outer curved surface. This reduces long path breakdown and spatially defines the plasma by restricting the current path to the exposed metal front face. A linear actuator is used to give accurate remote control of anode position (d), and thus gap. Axial resolution of +/-12μm is achievable over a wide range (1mm > d > 10mm).

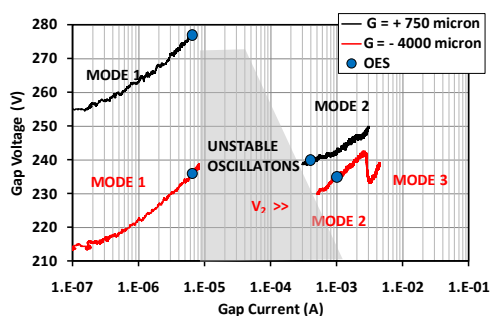


**Figure 2: Discharge Modes**

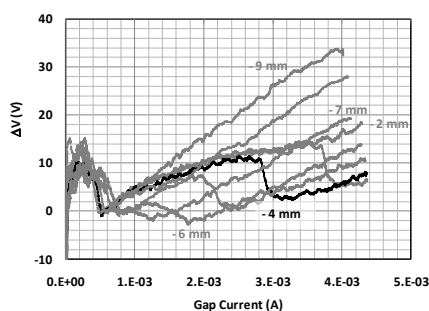


**Figure 3: Mode 3 onset**

The VI measurements Fig (2) clearly show distinct modes of discharge operation. At gap current  $I_{gap} < 10 \mu\text{A}$ , VI curves exhibit positive slopes differing only by a shift in breakdown voltages for external and internal anodes [4], and are shown as Mode 1. For  $10 \mu\text{A} < I_{gap} < 300 \mu\text{A}$ , an unstable oscillating regime [5] is observed. Above this current, stable operation is possible in Mode 2, where  $I_{gap}$  rises with  $V_{gap}$  for both anode positions.

However, the internal anode VI characteristic exhibits a sudden change at  $\sim 3$  mA. This onset of “Mode 3” occurs at progressively lower gap currents as the anode position approaches the far end of the cathode (Fig (3)). Thus Mode 3 is associated with the cathode end and Mode 2 can reach all along the cathode, its length a function of current and/or voltage.

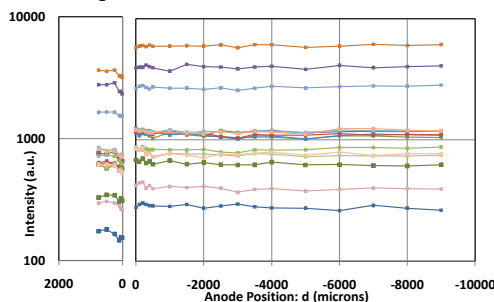


**Figure 4: Line Intensities vs Anode Position**

OES of Mode 2 discharges were performed at fibre optic positions A and B, Fig (1), for a wide range of  $d$ . Gap currents were 0.4 mA ( $d > 0$ ) and 1.0 mA ( $d < 0$ ). The total intensity at position A ( $I_A$ ) was near constant for all  $d$  whereas the intensity at B ( $I_B$ ) dropped markedly for  $750 \mu\text{m} > d > -500 \mu\text{m}$ .  $I_A \sim 3 I_B$  at maximum  $I_B$ . Individual argon line intensities for this range of  $d$  are shown in Fig (4). Again there is very little variation in Mode 2 for internal anode positions. External anodes display similar argon emission line ranking but with a drop in intensity for anode positions close to the cathode. The difference in intensities between external and internal data is because of the increase in  $I_{\text{gap}}$ .

Visual observation of the discharge geometry and extent is limited to the cathode face at  $d=0$  mm, however these do offer some indication of discharge geometries for external anodes. In Mode 1 an annular-cone shaped discharge is visible linking the anode and cathode faces/edges and in Mode 2 a disk shaped discharge is seen at the entrance to the cathode. The Mode 2 VI characteristics, Fig (3), suggest that the discharge can extend through the cathode, and one might expect it to be visible at the cathode face at  $d = -10$  mm. As previously noted, this face is not visible.

From these observations we can propose likely discharge geometries inside the cathode tube where direct observation is not possible. For  $I_{\text{gap}} < 10 \mu\text{A}$ , we assume the Mode 1 annular cone discharge becomes ring shaped for  $d < 0$  mm. The disk seen for  $I_{\text{gap}} > 300 \mu\text{A}$ , Mode 2, is assumed to extend longitudinally with increasing  $I_{\text{gap}}$ , towards the cathode face at  $d = -10$  mm where the transition to Mode 3 may occur. Possible explanations of the observed discharge behaviour are being considered including: longitudinal and radial diffusion of charged particles (initial calculations suggest electron densities of  $\sim 10^{14} \text{ cm}^{-3}$ ) and the formation of a virtual anode. Further characterisation and investigations into several of these interesting source aspects, including: OES of Mode2/3 onset, determination of excitation [6,7] and gas temperature, the use of a perforated cathode tube for radial OES access are ongoing. Other configurations including geometry and drive will allow comparative studies.

1. Bager, N., A. Bogaerts, and R. Gijbels, Spect. Acta Part B: 2002. **57**(2): p. 311-326.
2. McLaughlin, J.A. and P.D. Maguire, Diamond and Related Materials, 2008. **17**(4-5): p. 873-877.
3. Mariotti, D., J.A. McLaughlin., and P. Maguire., Plasma Sources Sci. Technol, 2004. **13**: p. 207-212.
4. Greenan J., Mahony C.M.O. & Maguire P.D., Bull Am Phys Soc 2009, **54**, 12 p45
5. Aubert., X., et al. Plasma Sources Sci. Technol., 2007. 16: p. 23-32.
6. Mariotti D. et al., Journal of Applied Physics, 2007. 101(1): p. 013307.
7. Mahony CMO, Gans T, Graham WG, Maguire PD & Petrovic Z Lj. APL, **93**, 011501 (2008)